

## Transition from Static to Dynamic Jahn-Teller Effects as Exhibited by the EPR Spectra of $\text{Ag}^{2+}$ in $\text{SrO}$ , $\text{CaO}$ , and $\text{MgO}$ †

L. A. Boatner and R. W. Reynolds

*Advanced Technology Center, Inc.,\* Dallas, Texas 75222*

and

M. M. Abraham and Y. Chen

*Oak Ridge National Laboratory, Oak Ridge, Tennessee 37830*

(Received 16 April 1973)

EPR investigations of  $\text{Ag}^{2+}$  in the series of isomorphous hosts  $\text{SrO}$ ,  $\text{CaO}$ , and  $\text{MgO}$  show that the low-temperature Jahn-Teller effect is static for  $\text{SrO}:\text{Ag}^{2+}$ , predominantly static but intermediate to the dynamic effect for  $\text{CaO}:\text{Ag}^{2+}$ , and predominantly dynamic but slightly intermediate to a static effect for  $\text{MgO}:\text{Ag}^{2+}$ . This represents the first observation of the systematic transition from static to dynamic Jahn-Teller effects at low temperature.

Theoretical treatments of the effects of Jahn-Teller (JT) coupling on EPR spectra associated with  ${}^2E$  electronic states have been given by O'Brien<sup>1</sup> for the case of strong Jahn-Teller coupling and by Ham<sup>2</sup> for the case of weak to moderate coupling. The principal features of the model arising from this work are as follows: For weak to moderate JT coupling the vibronic ground state remains a  ${}^2E$  state, and the first excited states are  $A_1$  and  $A_2$  levels which are accidentally degenerate for linear JT coupling. In what might be termed the "pure" dynamic regime, the first excited vibronic singlets are sufficiently removed from the ground state so that no observable interaction occurs between the  ${}^2E$  and  $A_1$  or  $A_2$  levels. For this case, the effects of JT coupling are manifested only in the form of reduced values for various perturbations which split the  ${}^2E$  state, and the associated EPR spectra are accurately described by second-order solutions of the effective Hamiltonian formulated by Ham.<sup>2</sup>

As the linear JT coupling increases, the  $A_1$  and  $A_2$  levels approach the ground state asymptotically. Additionally, nonlinear JT coupling terms ("warping" terms) can split the accidentally degenerate  $A_1$  and  $A_2$  levels. If the singlet-doublet energy separation is not large, appropriate perturbations (e.g., strain and anisotropic Zeeman interactions) can couple the singlet level to certain components of the random-strain-split ground state, and thus modify the observed EPR spectra.<sup>3</sup> When the linear JT coupling and warping terms are large, an  $A_1$  or  $A_2$  level approaches degeneracy with the ground state, and the "static" Jahn-Teller effect is observed. Chase<sup>3</sup> and Ham<sup>2</sup> have shown that the EPR spectra for  ${}^2E$

electronic states in cubic symmetry are strongly dependent on the ratio of the average random strain splitting  $\bar{\delta}$  to the  ${}^2E \rightarrow A_1$  or  $A_2$  splitting  $3\Gamma$  and that, in fact, the ratio  $\bar{\delta}/3\Gamma$  determines whether dynamic, static, or intermediate effects are observed.

Chase<sup>3</sup> has previously observed a selective shift and broadening of some components of the optically detected EPR spectrum for an excited  $\Gamma_8$  level of  $\text{Eu}^{2+}$  in  $\text{CaF}_2$ . The effects of strain coupling to an excited singlet level were responsible for these deviations from the predominantly dynamic features of this system. The work reported here for the  $\text{MgO}:\text{Ag}^{2+}$  system represents the second observation of this "quasidynamic"<sup>4</sup> JT effect. Features of EPR spectra corresponding to the alternate intermediate situation (i.e., a predominantly static system which is significantly affected by deviations from the limiting case of degeneracy of an  $A$  and  ${}^2E$  level) are reported here for the first time for the  $\text{CaO}:\text{Ag}^{2+}$  system. Additionally, the explanation of the  $\text{Ag}^{2+}$  EPR spectra in  $\text{SrO}$ ,  $\text{CaO}$ , and  $\text{MgO}$  represents the initial verification of the theory formulated by Chase<sup>3</sup> and Ham<sup>2</sup> to describe the transition from dynamic to static JT effects in the strong-coupling limit.

The silver-doped alkaline-earth oxide crystals used in the EPR investigations were grown by an arc-fusion technique.<sup>5</sup> Divalent silver has a  $[\text{Kr}]4d^9$  electronic configuration and a  ${}^2E$  orbital ground state in a sixfold coordinated cubic-symmetry site. EPR spectra due to  $\text{Ag}^{2+}$  were not observed in the "as-grown" single crystals, but could be obtained after room-temperature ultraviolet irradiations of about 4 h duration.

TABLE I.  $\text{Ag}^{2+}$  EPR parameters at 1.3 K.

Host	$\bar{\delta}/3\Gamma$	$g_{\parallel}$	$g_{\perp}$	Static Jahn-Teller effect			
				$^{107}\text{A}_{\parallel}$ ( $10^{-4} \text{ cm}^{-1}$ )	$^{109}\text{A}_{\parallel}$ ( $10^{-4} \text{ cm}^{-1}$ )	$^{107}\text{A}_{\perp}$ ( $10^{-4} \text{ cm}^{-1}$ )	$^{109}\text{A}_{\perp}$ ( $10^{-4} \text{ cm}^{-1}$ )
SrO	...	$2.112 \pm 0.001$	$2.017 \pm 0.001$	$28.79 \pm 0.02$	$33.31 \pm 0.02$	$22.92 \pm 0.02$	$26.61 \pm 0.02$
CaO	$1.2^a$	$2.166 \pm 0.001$	$2.031 \pm 0.001$	$29.4 \pm 0.4$	$34.0 \pm 0.4$	$21.0 \pm 0.3$	$24.8 \pm 0.3$

Host	$\bar{\delta}/3\Gamma$	$g_1$	$g_2$	Dynamic Jahn-Teller effect	
				$A_1$ ( $10^{-4} \text{ cm}^{-1}$ )	$qA_2$ ( $10^{-4} \text{ cm}^{-1}$ )
MgO	0.13	$2.0998 \pm 0.0007$	$+0.0563 \pm 0.0007$	$\pm 25.8 \pm 0.2^b$	$\pm 5.4 \pm 0.8^b$

<sup>a</sup>Obtained by fitting the spectrum observed at 8.8 GHz.

<sup>b</sup>The effective hyperfine parameters  $A_1$  and  $A_2$  given here are not to be confused with the labels  $A_1$  and  $A_2$  which are used to designate the excited singlet levels. The  $^{107}\text{Ag}$  and  $^{109}\text{Ag}$  isotopes were not resolved for orientations other than  $\vec{H} \parallel \langle 111 \rangle$ . The errors shown here were determined by assuming an experimental accuracy equal to 10% of the composite linewidth due to both isotopes.

At 1.3 K the EPR spectrum of  $\text{Ag}^{2+}$  in SrO consisted of three spectra with tetragonal symmetry and principal axes along  $\langle 100 \rangle$  directions. The spectra were characterized by symmetric line shapes, and the linewidth ( $\approx 1$  G) allowed good resolution of the hyperfine structure due to the  $^{107}\text{Ag}$  and  $^{109}\text{Ag}$  isotopes ( $I = \frac{1}{2}$ ). The tetragonal-symmetry spectra were described by the usual axially symmetric spin Hamiltonian, and the parameters  $g_{\parallel}$ ,  $g_{\perp}$ ,  $A_{\parallel}$ , and  $A_{\perp}$  determined for the  $\text{SrO}:\text{Ag}^{2+}$  system are given in Table I. As the sample temperature increased from 1.3 K, the anisotropic spectra decreased in intensity and were replaced by an isotropic, motionally averaged,  $\text{Ag}^{2+}$  spectrum. At 233 K only the isotropic spectrum could be observed; however, very weak vestiges of the tetragonal spectra were still present at 200 K. For the isotropic spectrum, a value of  $g = 2.047 \pm 0.002$  was determined experimentally. In the static JT limit the averaged spectrum is expected to occur at  $g = \frac{1}{3}(g_{\parallel} + 2g_{\perp})$ , where  $g_{\parallel}$  and  $g_{\perp}$  characterize the low-temperature anisotropic spectra. Using the measured values of  $g_{\parallel}$  and  $g_{\perp}$ , a  $g$  value of 2.049 is predicted. All of the features described above characterize what we have chosen to term the "pure" static Jahn-Teller case.<sup>4</sup>

At 1.3 K the EPR spectrum observed for  $\text{Ag}^{2+}$  in CaO also consisted of three  $\langle 100 \rangle$  axially symmetric spectra; however, the line shapes were asymmetric (see Fig. 1) and generally resembled the "powderlike" line shapes observed for systems exhibiting the low-temperature dynamic JT effect.<sup>6,7</sup> The angular dependence near the  $[111]$

direction of the  $\text{CaO}:\text{Ag}^{2+}$  spectrum is illustrated in Fig. 1, and the degeneracy of the observed

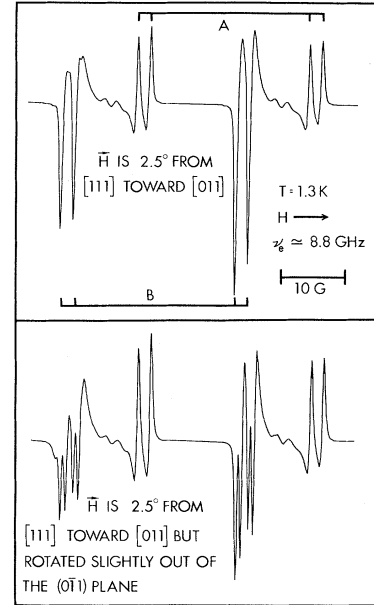


FIG. 1. Orientation dependence of the  $\text{Ag}^{2+}$  EPR spectrum in CaO. Top: groupings designated by A and B differentiate the spectra resulting from sites which are inequivalent in the  $(0\bar{1}1)$  plane. The doubling of each line results from the slightly different nuclear magnetic moments of  $^{107}\text{Ag}$  and  $^{109}\text{Ag}$  each of which has  $I = \frac{1}{2}$ . Bottom: the splitting of the "B" group into its two components indicates that the spectrum exhibits a static JT effect. Small lines due to averaging are seen between the high- and low-field components of each hyperfine group.

lines is clearly established. The angular variation was exactly described by an axial spin-Hamiltonian with the parameters listed in Table I.

The EPR spectra observed at 8.8 and 23 GHz with the applied dc magnetic field precisely oriented along a  $\langle 111 \rangle$  direction are shown in Fig. 2. At 8.8 GHz each hyperfine component of the  $^{107}\text{Ag}$  and  $^{109}\text{Ag}$  isotopes exhibits an unusual line shape. At 23 GHz the line shape consists of a large component with a reasonably conventional shape and a small component occurring at higher field with an asymmetric shape. (At 23 GHz note that the asymmetric component for the  $^{109}\text{Ag}$  isotope is also at the high-field side of the relatively large symmetric component associated with the  $^{107}\text{Ag}$  isotope.) Between 4.2 and 1.3 K the relative intensity of the symmetric and asymmetric components is unchanged, indicating that the observed high-field structure does not result from thermal population of an excited state or from averaging by relaxation between strain-split levels. The extra high-field structure at both frequencies occurs at the "average  $g$ -value" field position  $g = \frac{1}{3}(g_{\parallel} + 2g_{\perp})$ , while the main (low-field) resonance occurs at the field position expected for an axial spectrum with  $\vec{H} \parallel [111]$ , i.e.,  $g = [\frac{1}{3}(g_{\parallel}^2 + 2g_{\perp}^2)]^{1/2}$ . The observed line shapes are apparently characteristic of the intermediate state between the pure dynamic case and the pure

static case. We have shown that, with the technique described below, the line shapes can be related to the relative strengths of strain and JT coupling.

Using the technique described by Chase,<sup>3</sup> a computer diagonalization was made of the matrix of strain and JT coupling interactions between the  $A_2$  and  ${}^2E_g$  states. (Since  $g_{\parallel} > g_{\perp}$ , it can be argued that the  $A_2$  level is nearest the  ${}^2E_g$  ground state.<sup>3</sup>) The diagonalizations were carried out for strains which had a Gaussian distribution about an rms strain  $\bar{\delta}$  and which were randomized between  $e_{\theta}$  and  $e_{\epsilon}$  components. Expectation values of the Zeeman and hyperfine interactions were computed from the eigenvectors resulting from each diagonalization. The resulting computed EPR spectrum at 8.8 GHz duplicated the observed line shape for  $\vec{H} \parallel [111]$  when the ratio  $\bar{\delta}/3\Gamma$  was 1.2. The  $\text{CaO}:\text{Ag}^{2+}$  system is typical of what we term the "quasistatic" Jahn-Teller effect.

The EPR spectrum observed at 1.3 K for  $\text{Ag}^{2+}$  in  $\text{MgO}$  is characterized by an angular variation somewhat similar to that obtained for  $\text{Y}^{2+}$  in  $\text{SrCl}_2$ ,<sup>6</sup> which is a system exemplifying what we term the "pure dynamic" JT case. The effects of selective coupling to an excited singlet  $A_2$  level<sup>3</sup> are observed for the  $\text{MgO}:\text{Ag}^{2+}$  system, however. For orientations of the applied magnetic field in a  $(1\bar{1}0)$  plane other than  $\vec{H} \parallel [111]$ , the  $\text{Ag}^{2+}$  spectrum consisted of two hyperfine sets, and one of these was appreciably sharper than the other. In the  $(1\bar{1}0)$  plane the "sharp" components cross from the high-field side of the spectrum to the low-field side as the magnetic field orientation is changed from  $\vec{H} \parallel [001]$  to  $\vec{H} \parallel [110]$ . For  $\vec{H} \parallel [001]$  the "broad" components are shifted to a lower field position than that predicted by second-order solutions<sup>7</sup> to Ham's effective spin Hamiltonian for a  ${}^2E$  state with the parameters which describe the angular variation of the "sharp" components. Using the computer technique noted previously to include the interaction with the  $A_2$  level, it was possible to fit the complete angular variation with a value of  $\bar{\delta}/3\Gamma = 0.13$ , and the parameters given in Table I (values of  $q = \frac{1}{2}$  and  $r = -\sqrt{2}q$  were assumed, where  $q$  and  $r$  are the parameters defined by Ham<sup>2</sup> and Chase<sup>3</sup>).

At 4.2 K an intense isotropic spectrum is observed which coincides with the field positions of the anisotropic components when the applied field is parallel to a  $\langle 111 \rangle$  direction. Since the ratio  $\bar{\delta}/3\Gamma$  indicates that the  $A_2$  state is close to the ground  ${}^2E$  level, and since the observed intensity of the isotropic spectrum is a distinctly

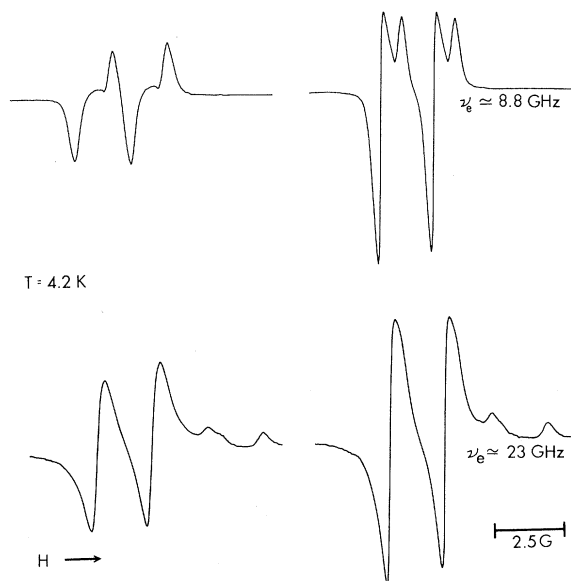


FIG. 2. EPR spectrum of  $\text{Ag}^{2+}$  in  $\text{CaO}$  with  $\vec{H} \parallel [111]$ . The top trace was taken at a frequency of 8.8 GHz and the bottom trace at 23 GHz. The line shapes result from intermediate JT coupling effects.

nonlinear function of temperature, it is reasonable to assume that a significant portion of this intensity is due to thermal population of the singlet. Assuming then that the intensity varies as  $\exp(-3\Gamma/kT)$ , which is also valid for averaging by relaxation via an Orbach process, we can calculate a value of  $3\Gamma = 4.8 \text{ cm}^{-1}$  from the intensity variations observed between 4.2 and 1.3 K. This value and the value of  $\bar{\delta}/3\Gamma = 0.13$  are then used to calculate an average strain splitting  $\bar{\delta}$  of  $0.62 \text{ cm}^{-1}$ . An average strain splitting of the orbital doublet on the order of  $1.0 \text{ cm}^{-1}$  has previously been estimated by Ham.<sup>2</sup> The features of the EPR spectrum of  $\text{Ag}^{2+}$  as described above are characteristic of what we term<sup>4</sup> the "quasidynamic" JT effect.

The EPR spectra of  $\text{Ag}^{2+}$  reported here for the three alkaline-earth oxide hosts  $\text{SrO}$ ,  $\text{CaO}$ , and  $\text{MgO}$  illustrate the transition from a case very close to the static limit ( $\text{SrO}:\text{Ag}^{2+}$ ) to a case which is predominantly static, but in transition to the dynamic situation ( $\text{CaO}:\text{Ag}^{2+}$ ), and finally to a case which is essentially dynamic ( $\text{MgO}:\text{Ag}^{2+}$ ), but for which the proximity of an excited singlet level produces significant departures from the spectrum expected for an isolated  ${}^2E$  level. In each case, the formalism of Ham<sup>2</sup> and Chase<sup>3</sup> which describes the transition from dynamic to

static JT effects at low temperature satisfactorily explains all major features of the spectrum.

The authors are particularly indebted to L. L. Chase for the correspondence regarding his computer analysis of intermediate coupling effects, and acknowledge helpful discussions with F. S. Ham and T. L. Estle.

---

†Research sponsored in part by the U. S. Atomic Energy Commission under contract with Union Carbide Corporation.

\*P. O. Box 6144.

<sup>1</sup>M. C. M. O'Brien, Proc. Roy. Soc. Ser. A **281**, 1356 (1964).

<sup>2</sup>F. S. Ham, Phys. Rev. **166**, 307 (1968). See also F. S. Ham, in *Electron Paramagnetic Resonance*, edited by S. Geschwind (Plenum, New York, 1971).

<sup>3</sup>L. L. Chase, Phys. Rev. B **2**, 2308 (1970).

<sup>4</sup>Although theoretically a continuous range of possibilities exists between the two limits "pure" static and "pure" dynamic, the great differences in the experimentally observed EPR spectra make "quasistatic" and "quasidynamic" useful classifications.

<sup>5</sup>M. M. Abraham, C. T. Butler, and Y. Chen, J. Chem. Phys. **55**, 3752 (1971).

<sup>6</sup>J. R. Herrington, T. L. Estle, and L. A. Boatner, Phys. Rev. B **7**, 3003 (1973).

<sup>7</sup>J. R. Herrington, T. L. Estle, and L. A. Boatner, Phys. Rev. B **3**, 2933 (1971).

---

## Hot-Electron Plasma Confinement in the Superconducting Levitron\*

O. A. Anderson, D. H. Birdsall, C. W. Hartman, E. B. Hooper, Jr., and R. H. Munger

*Lawrence Livermore Laboratory, University of California, Livermore, California 94550*

(Received 9 April 1973)

Cyclotron resonance heating is used to produce hot ( $T \approx 250 \text{ keV}$ ) electrons with  $\beta$  up to 10% in an axisymmetric torus. The plasma pressure is nearly isotropic. Confinement times of several seconds are achieved, limited by collisions with background gas. Plasma stability is described.

An efficient toroidal fusion reactor must operate at a substantial value (approaching 10%) of  $\beta \equiv nkT(B^2/8\pi)^{-1}$ . In such a reactor, with  $T_{\text{ion}} \geq 20 \text{ keV}$ , the ion mean free path is much larger than the plasma dimension associated with mirror trapping. One would expect plasma behavior in this regime to be qualitatively different from the low- $\beta$  collisional case representative of most present-day toroidal confinement experiments. For example, in the tokamak configuration under reactor conditions, theory predicts trapped-particle instabilities including a hydromagneticlike mode<sup>1</sup> which could seriously impair confinement.

Unfortunately, it may be years before this sort of prediction can be checked experimentally in an actual tokamak.

Toroidal confinement of finite- $\beta$  collisionless plasma can be studied in the technically simpler situation where hot electrons, rather than hot ions, provide the pressure. This has previously been done using magnetic-mirror confinement and electron-cyclotron-resonance (ECR) heating.<sup>2</sup> In this Letter we report the first studies of the toroidal confinement of a hot-electron plasma having a large  $\beta$ . The experiments were conducted in the superconducting levitron.<sup>3</sup> Hot elec-